Supplementary Information (SI) for RSC Sustainability.
This journal is © The Royal Society of Chemistry 2024

Supporting Information

Photodegradation of Berberine Hydrochloride at the Interface of 1D-2D Nanohybrid of Nickel Ferrite supported on Reduced Graphene Oxide

Sayanika Saikia[a], Salma A. Khanam[a], Priyanuj Kandali[a], Ankur Kanti Guha[b], Kusum K. Bania[a]*

[a]*Department of Chemical Sciences, Tezpur University, Assam, India, 784028.*
[b]*Advanced Computational Chemistry Centre, Cotton University, Panbazar, Guwahati, Assam 781001, India.*

Corresponding Author
*****Email: kusum@tezu.ernet.in or bania.kusum8@gmail.com
ORCID
Kusum K. Bania: 0000-0001-6535-3913

1. Physical measurement

Physical measurements for different characterizations and analyses were done by the following techniques. The powder-X-ray diffraction (XRD) patterns were recorded in an instrument from BRUKER AXS, D8 FOCUS in the 2θ value range of 5–80°. Raman spectroscopy was carried out on RENISHAW BASIS SERIES WITH 514 LASERS (software: WIRE 3.4). The Diffuse Reflectance Spectra (DRS) were recorded employing a Hitachi U-3400 spectrophotometer. The infrared spectra had been recorded on a Perkin- Elmer 2000 FTIR spectrometer within the range of 450-4000 cm^{-1}. The spectra of the solid samples were recorded as KBr pellets through blending the samples with KBr. Thermogravimetric analysis was performed on simultaneous TG-DTA thermo analyzer, Mettler Toledo, under air atmosphere. Brunauer- Emmett-Teller (BET) surface areas were obtained by means of N_2 sorption data measured at 77 K by a volumetricadsorption setup (Autosor IQ-MP Make: Quantachrome, USA). Scanning Electron Microscope (SEM) images along with the X-Ray and Elemental mapping analyses were done ZEISS, SIGMA instrument manufactured by Carl Zeiss Microscopy. The Transmission Electron Microscope (TEM) images along with energy dispersive X-ray spectroscopy (EDX) analysis was performed on a JEM-2100 PlusElectron Mocroscope (JEOL). SEM-EDX analysis was done with JSM 6390LV, JEOL SOFTWARE (WINDOW BASED). Inductively Coupled Plasma Optical Emission Spectrophotometer (ICP-OES) analysis was performed in PERKIN ELMER, USA, Model: AVIO 220 MAX. The cyclic voltammetry (CV) and Mott Schottky (MS) analysis studies were performed in a CHI-600E meter from CH Instruments using the glassy carbon electrode (GCE) and Pt as a working electrode, Ag/AgCl as reference electrode and Pt wire as a counter electrode, respectively. PL spectra were recorded in FL3C-KIT_2031C-4819-FL instrument. The photoelectrochemical measurements of the samples

was carried out in a three-electrode working set up consisting of WE (Substrates), RE (Ag/AgCl) and CE (Pt wire),1 M KOH (model- CHI1120B). The X-ray photoelectron (XPS) spectra were obtained from a XPS KRATOS (ESCA AXIS 165) spectrometer having Mg Kα (1253.6 eV) as radiation source. Before transferring to the analysis chamber, the oven-dried sample was crushed into small pieces, sprinkled on a graphite sheet (double rod), and attached to a normal sample holder. The material was degassed overnight in a vacuum oven. The binding energy value was modified with reference to the 284.8 eV C 1s peak and the peak was deconvoluted using Origin software. The UV-Vis experiments were carried out in Shimadzu, UV-2550 spectrophotometer. 500 mL of quartz glass chamber with a Mercury lamp, light source was surrounded by a double jacked quartz immersion with an inlet and outlet of water circulation to ensure a safe temperature for the photocatalytic reaction**.** The mass of the intermediate molecules was determined by Low-resolution mass spectra (LRMS). Mass spectra (MS) of the samples were recorded in Thermo Scientific Q-Exactive, Accela 1250 pump. Electron spin resonance (ESR) spectroscopy was recorded in JEOL, Japan (JES - FA200 ESR Spectrometer with X and Q band).

2. Synthesis procedure of Fe_2O_3 and NiO.

I. Synthesis of Fe_2O_3

For the synthesis of Fe_2O_3, 0.01 M (0.135 g in 50 mL water) of iron (III) chloride solution was stirred at 60 ^oC. 50 mL of 0.1 M of sodium hydroxide (NaOH) solution was added dropwise to the above solution and refluxed for another 24 h. Resultant material was filtered, washed properly and then calcined at 400 ℃ for 5 h.

II. Synthesis of NiO

NiO was synthesized using simple precipitation method. A 0.1 M solution of $NiCl_2 \cdot 6H_2O$ was treated with a 0.1 M solution of NaOH to get a precipitate of $Ni(OH)_2$. The precipitate was filtered and washed with distilled water to get rid of unreacted components. Then the material was calcined at 400 ºC for 3 h to get NiO.

3. FTIR spectra of NFNR, rGO and NFNR/rGO

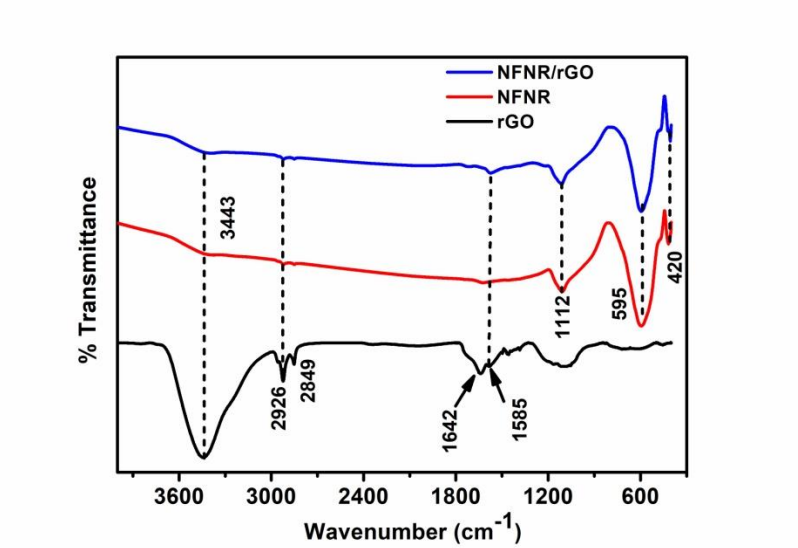

Fig. S1 FTIR spectra of of rGO (black), NFNR (red) and NFNR/rGO (blue).

4. TGA spectra of NFNR, rGO and NFNR/rGO

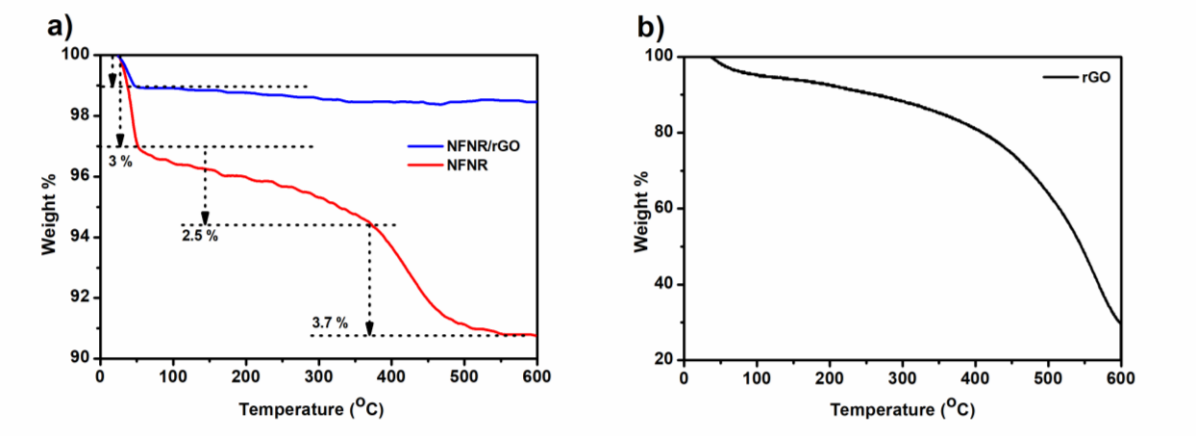

Fig. S2 TGA spectra of a) NFNR (red line) and NFNR/rGO (blue line) and b) rGO (black line).

5. N_2 adsorption-desorption isotherm of NFNR/rGO

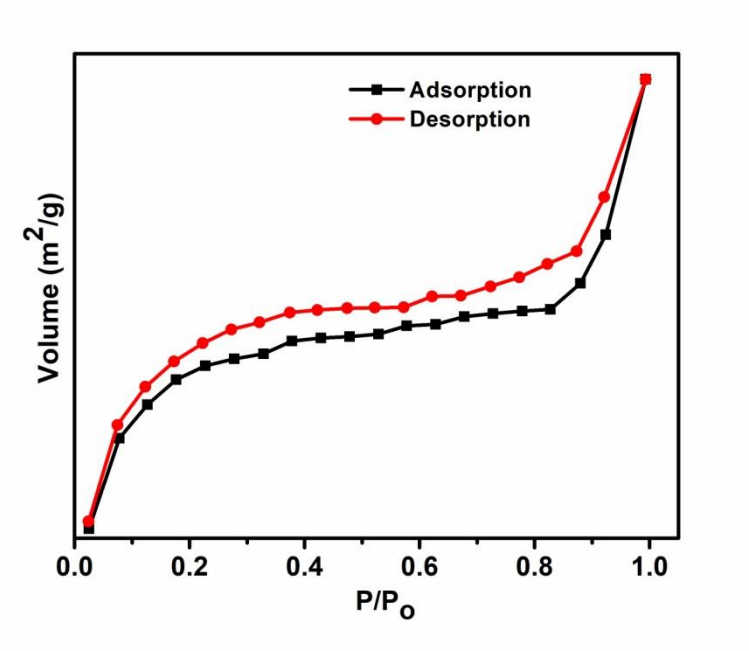

Fig. S3 N_2 adsorption-desorption isotherm of NFNR/rGO.

6. Nyquist plot of NFNR, rGO and NFNR/rGO

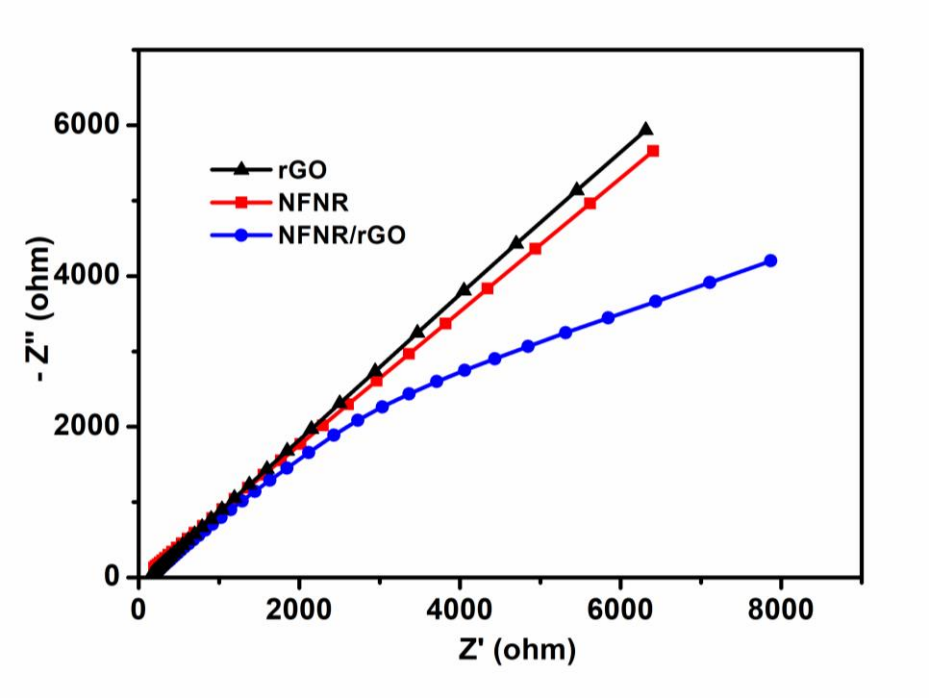

Fig. S4 Nyquist plot of NFNR (red line), NFNR/rGO (blue line) and rGO (black line).

7. UV spectra and bar diagram of BH degradation for different prepared catalysts.

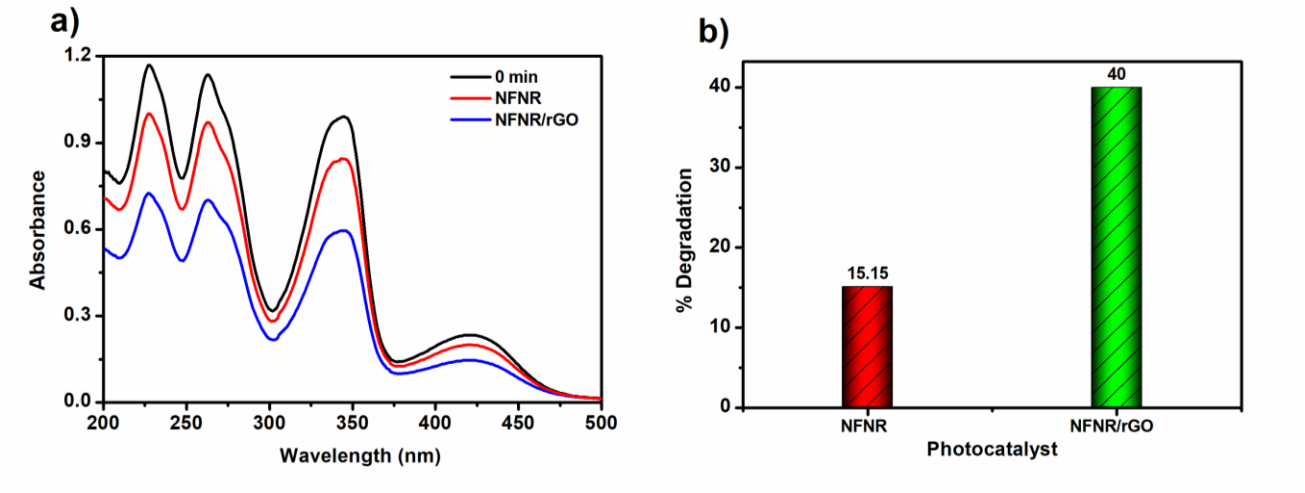

Fig. S5 a) UV spectra and b) bar diagram of BH degradation with NFNR and NFNR/rGO catalyst (2 mg) with 90 min UV-light irradiation at pH=2 (20 ml of 50 ppm BH solution).

8. UV spectra and bar diagram of BH degradation with NFNR/rGO for light irradiation condition.

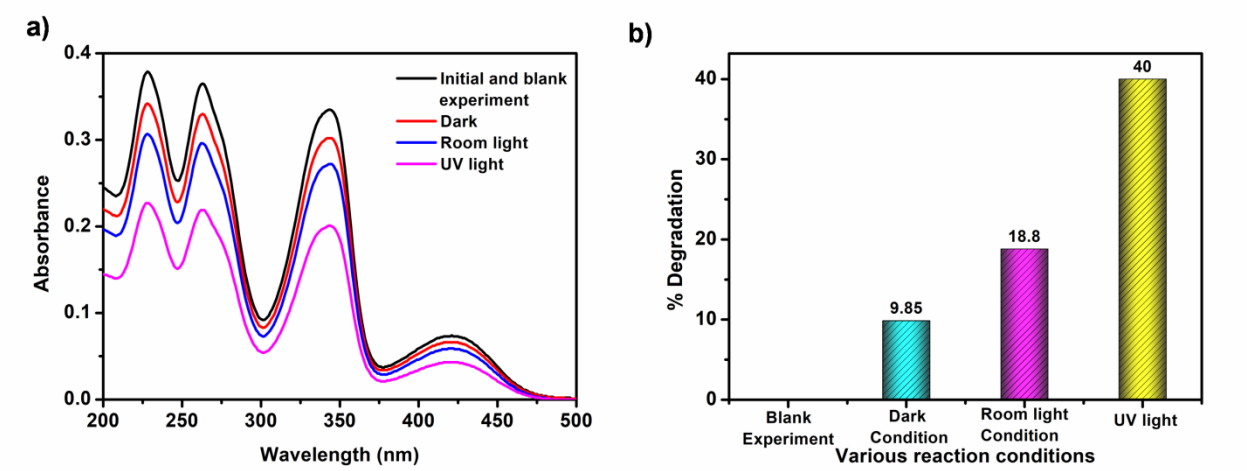

Fig. S6 a) UV spectra and b) bar diagram for comparison of BH degradation under dark, room light and UV light irradiation with NFNR/rGO (2 mg) catalyst, 90 min irradiation and pH=2.

9. Point of Zero Charge (pH_{PZC}) of NFNR/rGO

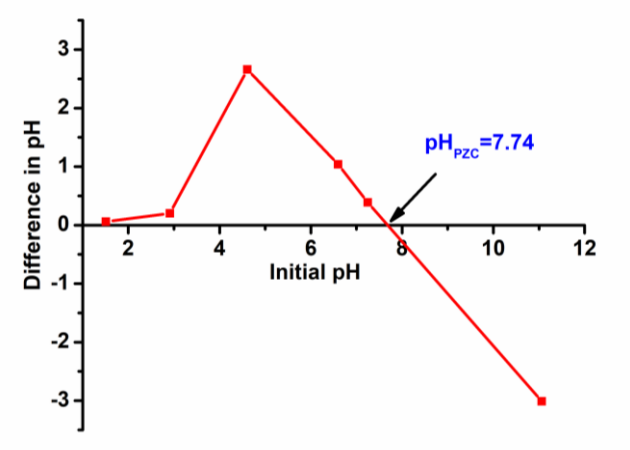

Fig. S7 Point of Zero Charge (pH_{PZC}) of NFNR/rGO.

10. Effect of initial pH of BH solution on photodegradation of BH

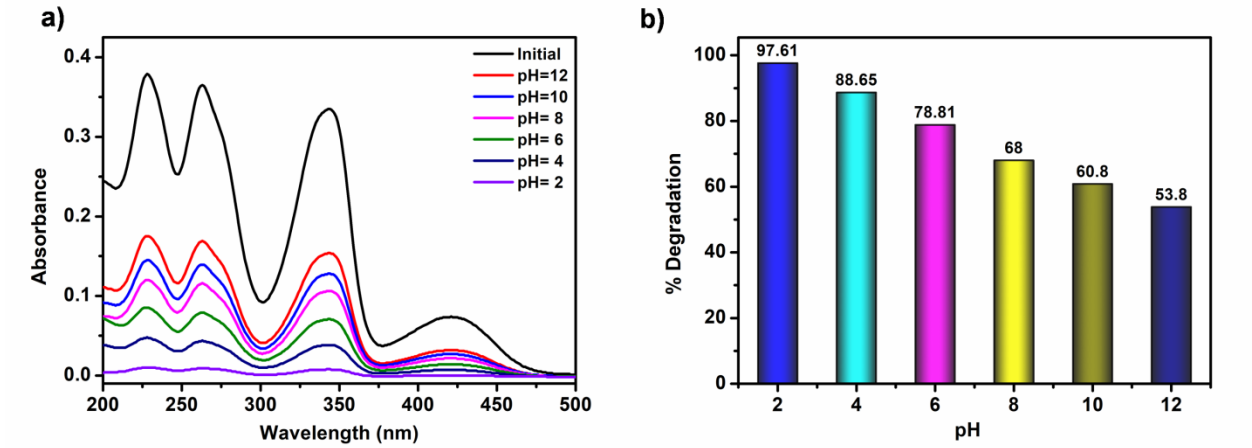

Fig. S8 a) UV spectra and b) bar diagram showing the effect of pH on BH degradation (20 ml of 50 ppm BH solution, 12 mg NFNR/rGO, and 60 min of UV light irradiation).

11. **UV spectra and bar diagram of BH degradation for different BH solution concentration**

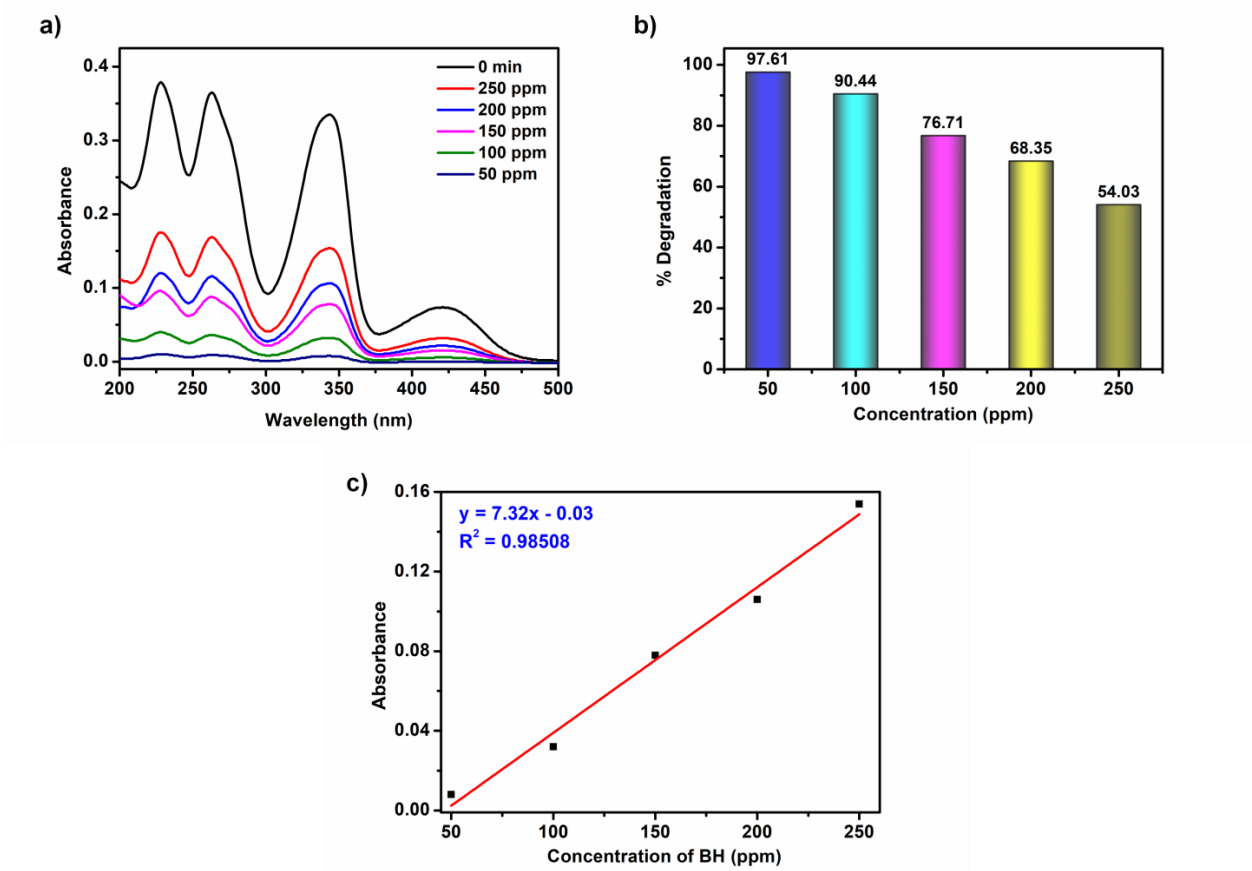

Fig. S9 a) UV spectra, b) bar diagram of BH degradation for different initial concentration of BH solution (12 mg catalyst, 60 min of irradiation time and pH=2) and c) linear relationship of absorbance vs. concentration of BH.

12. **Kinetic analysis of BH degradation**

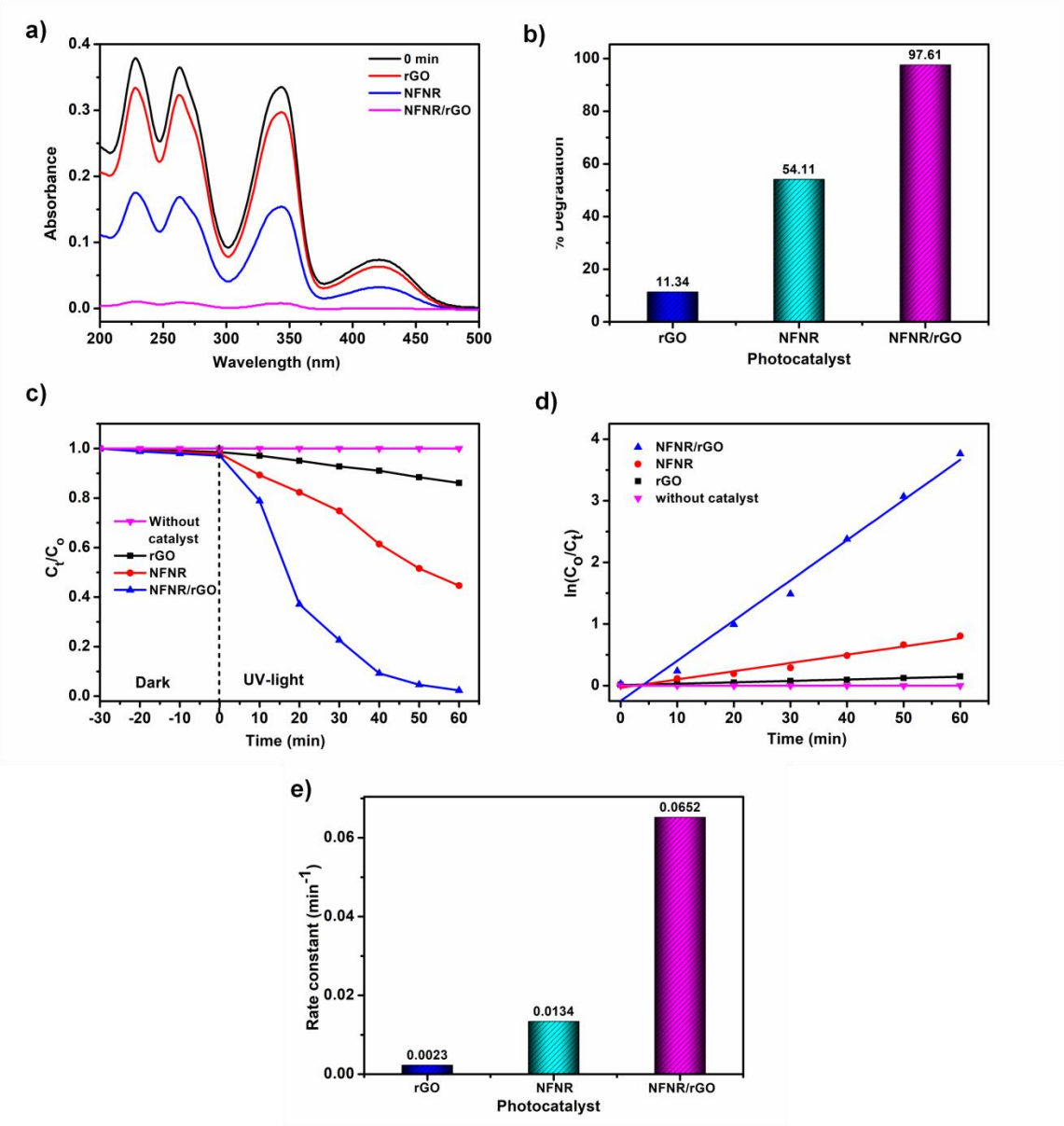

Fig. S10 a) UV spectra, b) bar diagram showing the degradation of BH with NFNR, rGO and NFNR/rGO (12 mg, 60 min irradiation and pH=2), c) time dependent degradation curve, d) corresponding photodegradation kinetic curves and e) rate constant of BH degradation over as-prepared samples.

13. Comparison of BH degradation efficiency of NFNR/rGO composite with physical mixture of NFNR and rGO

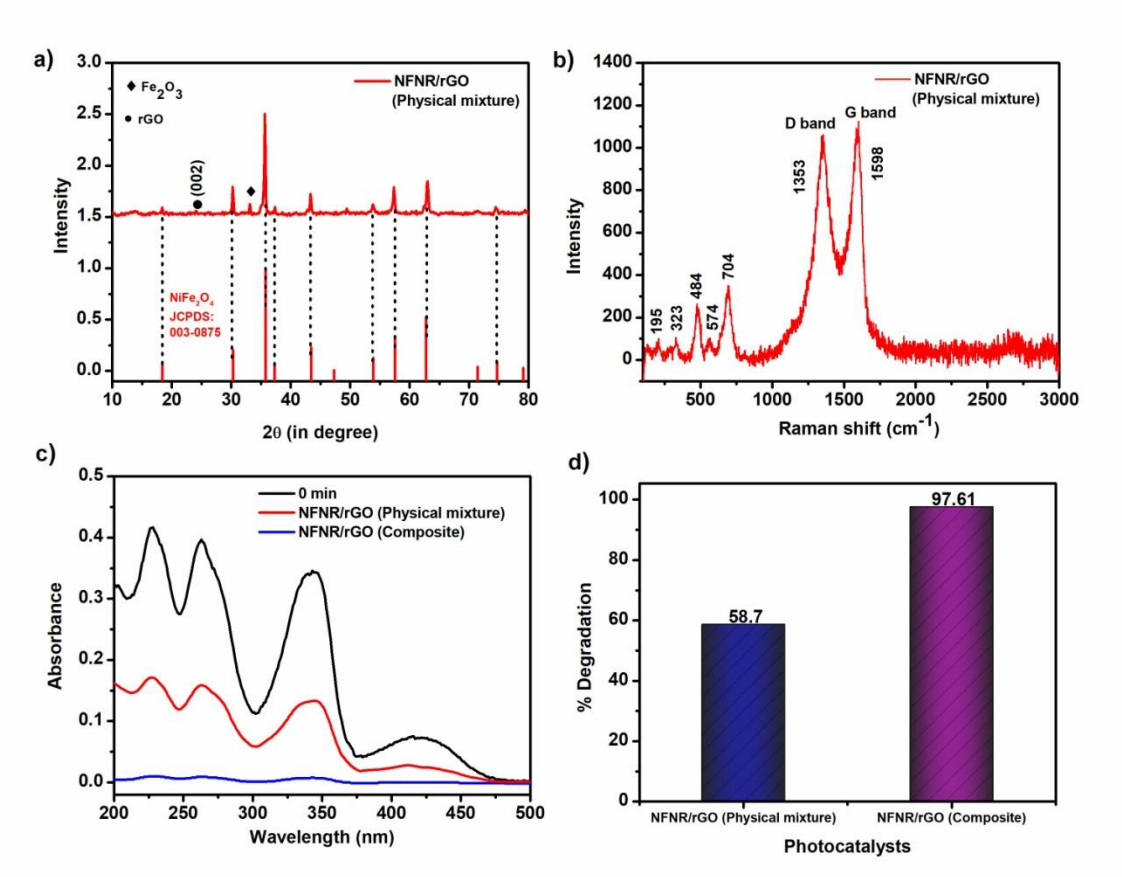

Fig. S11 a) PXRD and b) Raman analysis, c) UV spectra and d) bar diagram showing the comparision of BH degradation efficiency of NFNR/rGO composite with physical mixture of NFNR and rGO.

14. Percentage mineralization efficiency of BH

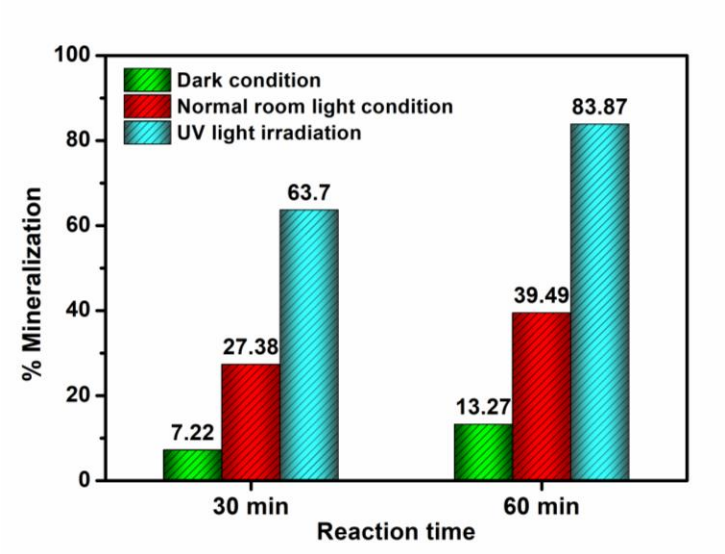

Fig. S12 Percentage of mineralization efficiency of BH using NFNR/rGO (12 mg) under dark, room light and UV light irradiation at different reaction time.

15. Stability test of NFNR/rGO under strong acidic condition (pH=2)

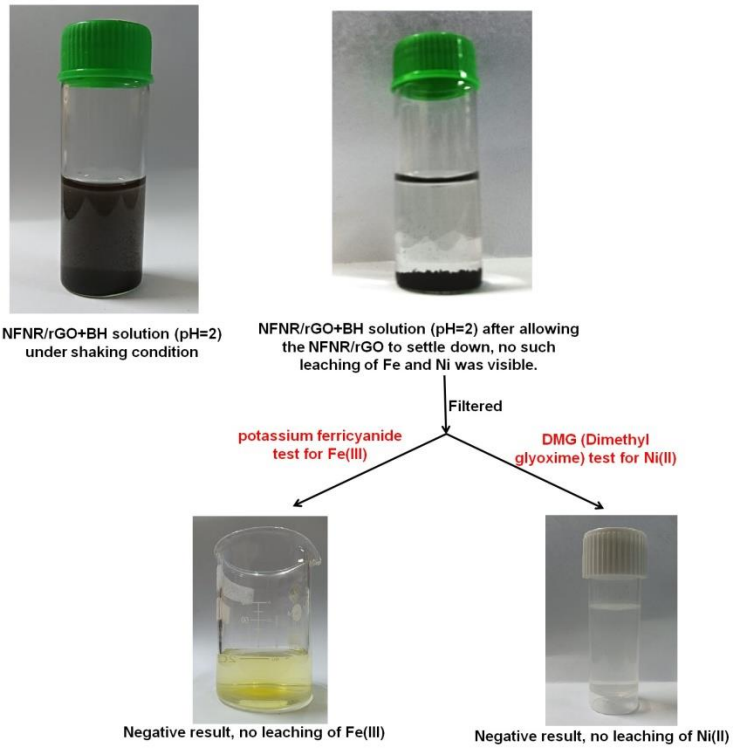

Fig. S13 Stability test of NFNR/rGO under strong acidic condition (pH=2)

16. BH degradation with various scavenging agents

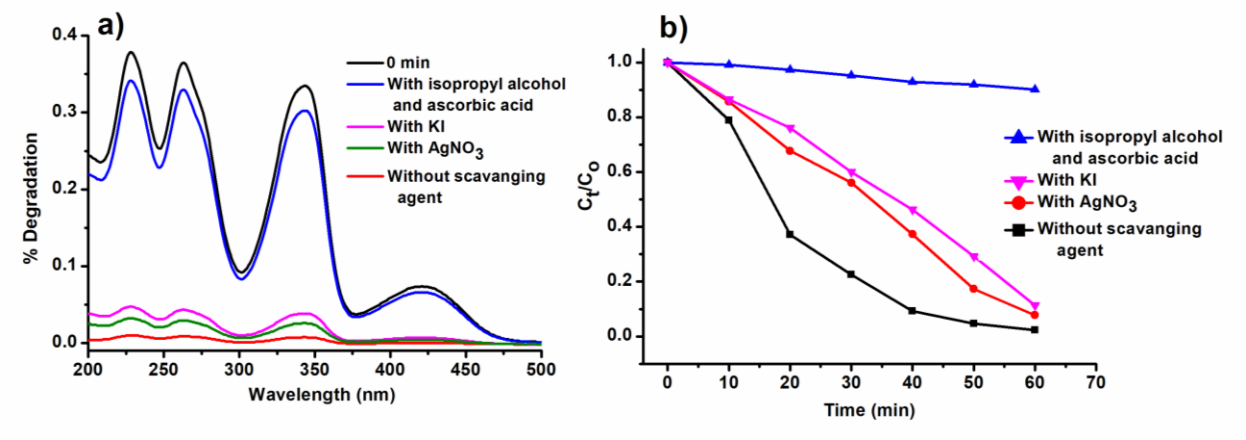

Fig. S14 a) UV graph and b) time dependent degradation curve for comparing the photocatalytic activity of NFNR/rGO for BH degradation (12 mg catalyst, 60 min of irradiation time and pH=2) with the addition of scavengers or without scavengers under optimized reaction conditions.

17. ESR analysis

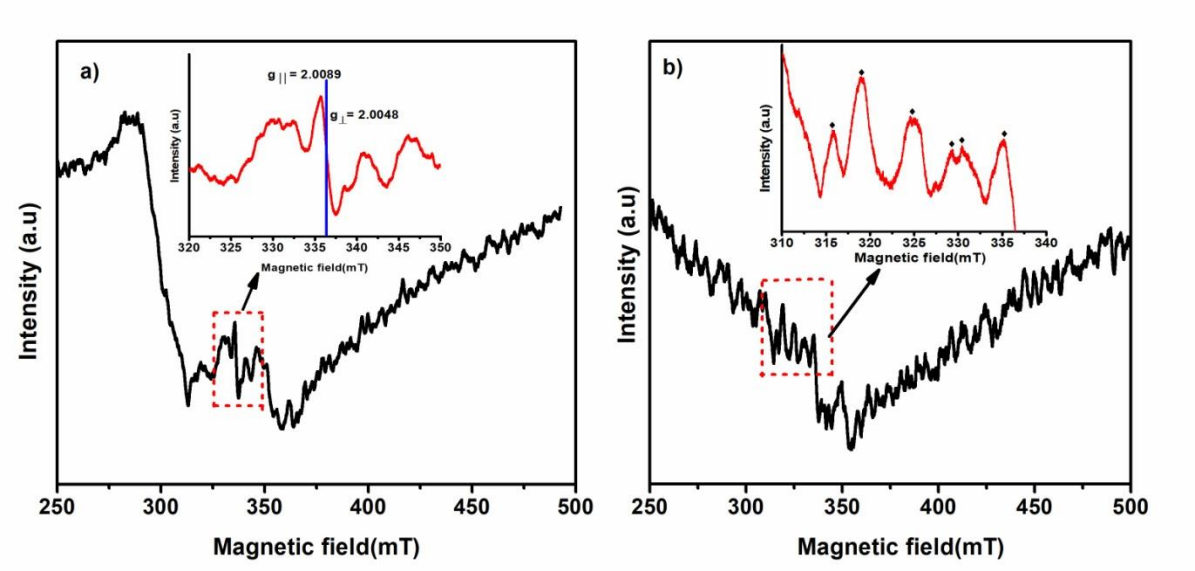

Fig. S15 ESR analysis a) before adding DMPO and b) after adding DMPO.

18. PXRD pattern of the other synthesized catalysts: NFNR-1/rGO, NFNR-2/rGO, NFNR/CTW, Fe_2O_3 and NiO

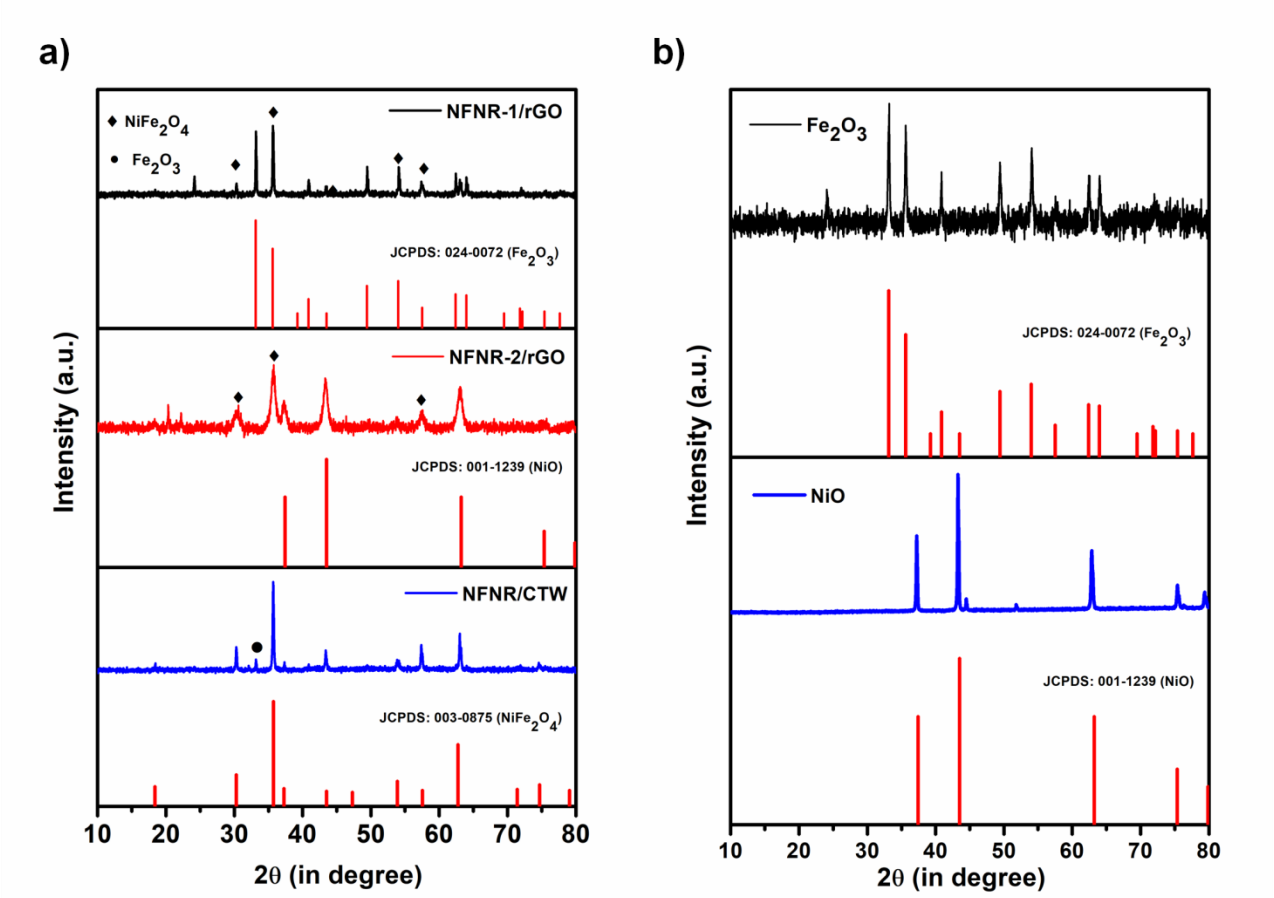

Fig. S16 PXRD pattern of synthesized catalysts: a) NFNR-1/rGO, NFNR-2/rGO, NFNR/CTW and b) Fe_2O_3, NiO.

19. Raman spectra of the other synthesized catalysts: NFNR-1/rGO, NFNR-2/rGO, NFNR/CTW, Fe_2O_3 and NiO

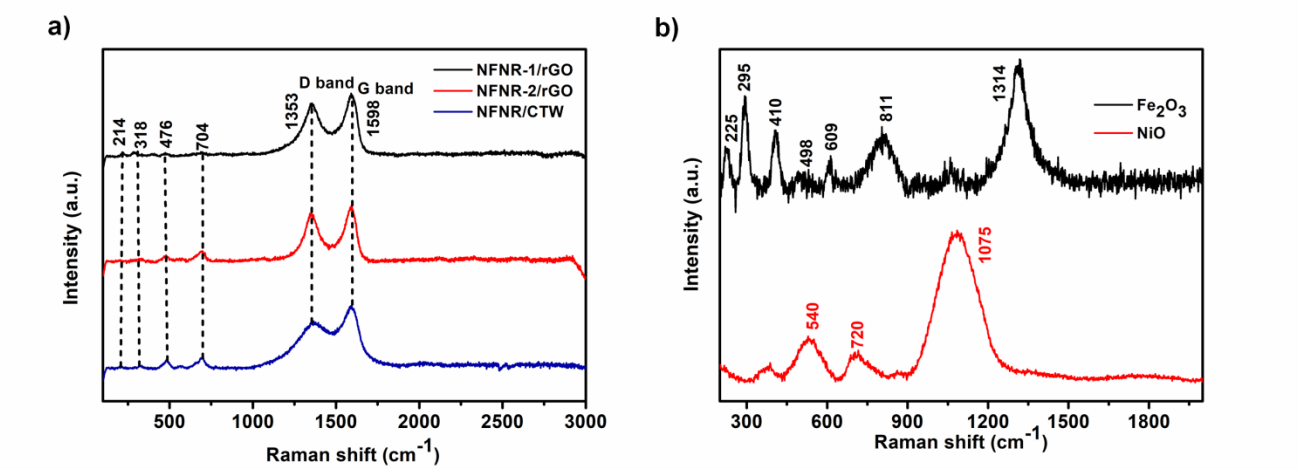

Fig. S17 Raman spectra of synthesized catalysts: a) NFNR-1/rGO, NFNR-2/rGO, NFNR/CTW and b) Fe_2O_3, NiO.

Table S1 Raman analysis of synthesized catalysts

Sl No.	Materials	Raman shift (cm^{-1})	Assignment	References
1	NFNR-1/rGO	214, 476	T_{2g} mode	1
	NFNR-2/rGO	318	E_g mode	1
	NFNR/CTW	704	A_{1g} mode	2
		1353	D-band	3
		1598	G-band	3
2	Fe_2O_3	225, 498	A_{1g} symmetry	4
		295, 410, 609, 811	E_g symmetry	5
		1360	Attributed to typical hematite	
3	NiO	540	one-phonon (1P) TO and LO modes	6
		720	two-phonon (2P) 2TO modes	
		1075	2LO modes	

20. FTIR spectra of the other synthesized catalysts: NFNR-1/rGO, NFNR-2/rGO, NFNR/CTW, Fe_2O_3 and NiO

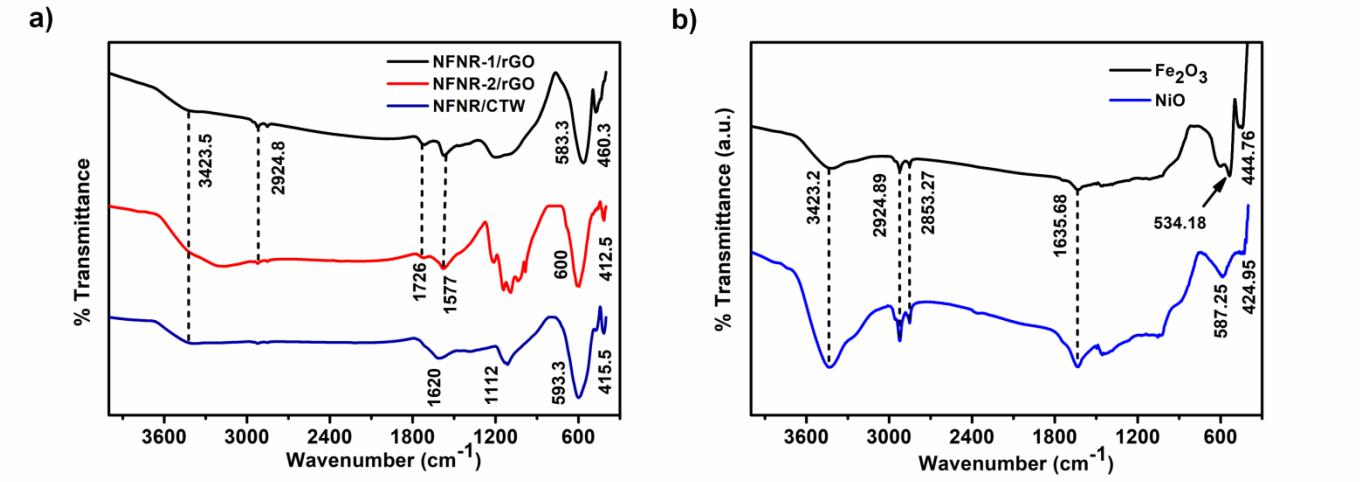

Fig. S18 FTIR spectra of synthesized catalysts: a) NFNR-1/rGO, NFNR-2/rGO, NFNR/CTW and b) Fe_2O_3, NiO.

Table S2 FTIR analysis of synthesized catalysts.

Sl no.	Materials	Wavenumber (cm^{-1})	Assignment	Reference
1	NFNR-1/rGO	460.3	ν_{Fe-O}	7
		583.3	ν_{Ni-O}	
		1577, 1726	-COOH, -C-OH, -C-O vibration	8
		2924.8	$\nu_{s(-C-H)}$	9
		3424.8	ν_{O-H}	10
2	NFNR-2/rGO	412.5	ν_{Fe-O}	7
		600	ν_{Ni-O}	
		1577, 1726	-COOH, -C-OH, -C-O vibration	8
		2924.8	$\nu_{s(-C-H)}$	9
		3424.8	ν_{O-H}	10
3	NFNR/CTW	415.5	ν_{Fe-O}	7
		593.3	ν_{Ni-O}	
		1112	ν_{C-O}	
		1620		
		3424.8	ν_{O-H}	
4	Fe_2O_3	534.18	ν_{Fe-O}	11
		1635.68, 3423.2	Surrface hydration	
		2924.89, 2853.27	$\nu_{as(C-H)}$	
5	NiO	424.95	ν_{Ni-O}	6

21. TGA pattern of the other synthesized catalysts: NFNR-1/rGO, NFNR-2/rGO and NFNR/CTW

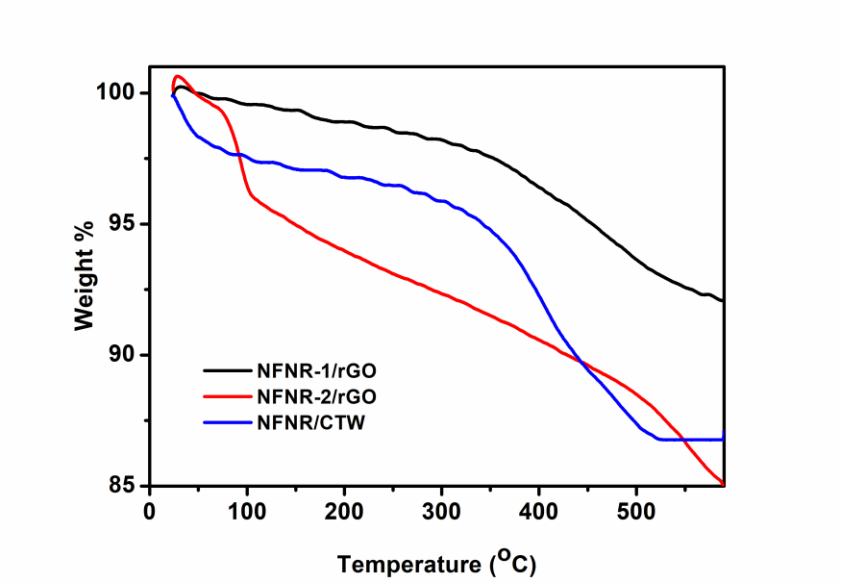

Fig. S19 TGA spectra of the NFNR-1/rGO, NFNR-2/rGO and NFNR/CTW.

22. SEM-EDX pattern of the other synthesized catalysts: NFNR-1/rGO, NFNR-2/rGO and NFNR/CTW

a)

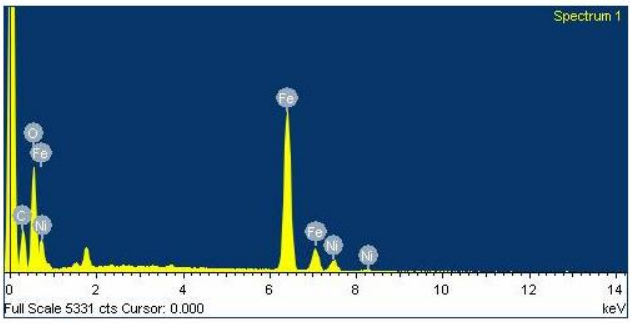

b)

Element	Weight %	Atomic %
C K	22.21	40.66
O K	29.36	40.35
Fe K	44.04	17.34
Ni K	4.40	1.65
Total	100	100

c)

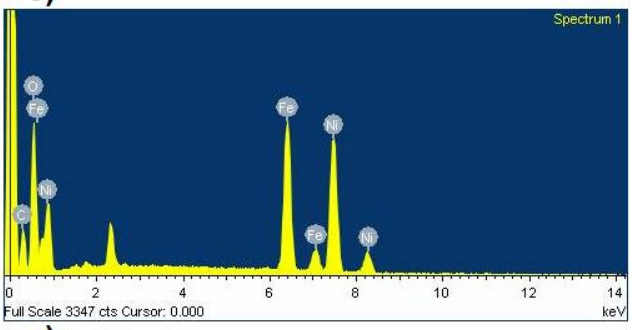

d)

Element	Weight %	Atomic %
C K	17.32	35.93
O K	25.14	39.14
Fe K	23.90	10.66
Ni K	33.64	14.27
Total	100	100

e)

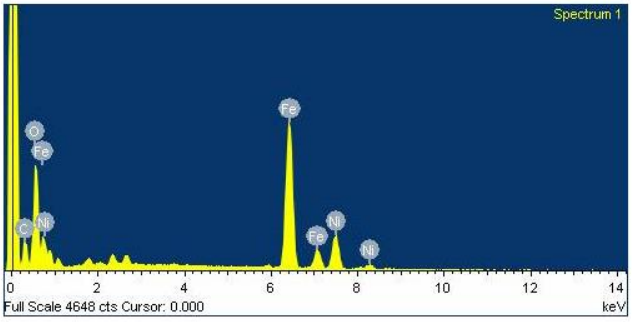

f)

Element	Weight %	Atomic %
C K	16.65	33.74
O K	27.86	42.38
Fe K	41.17	17.94
Ni K	14.32	5.94
Total	100	100

Fig. S20 SEM-EDX pattern of a), b) NFNR-1/rGO, c), d) NFNR-2/rGO and e), f) NFNR/CTW.

23. Photocatalytic degradation of BH with other synthesized catalyst under optimized conditions.

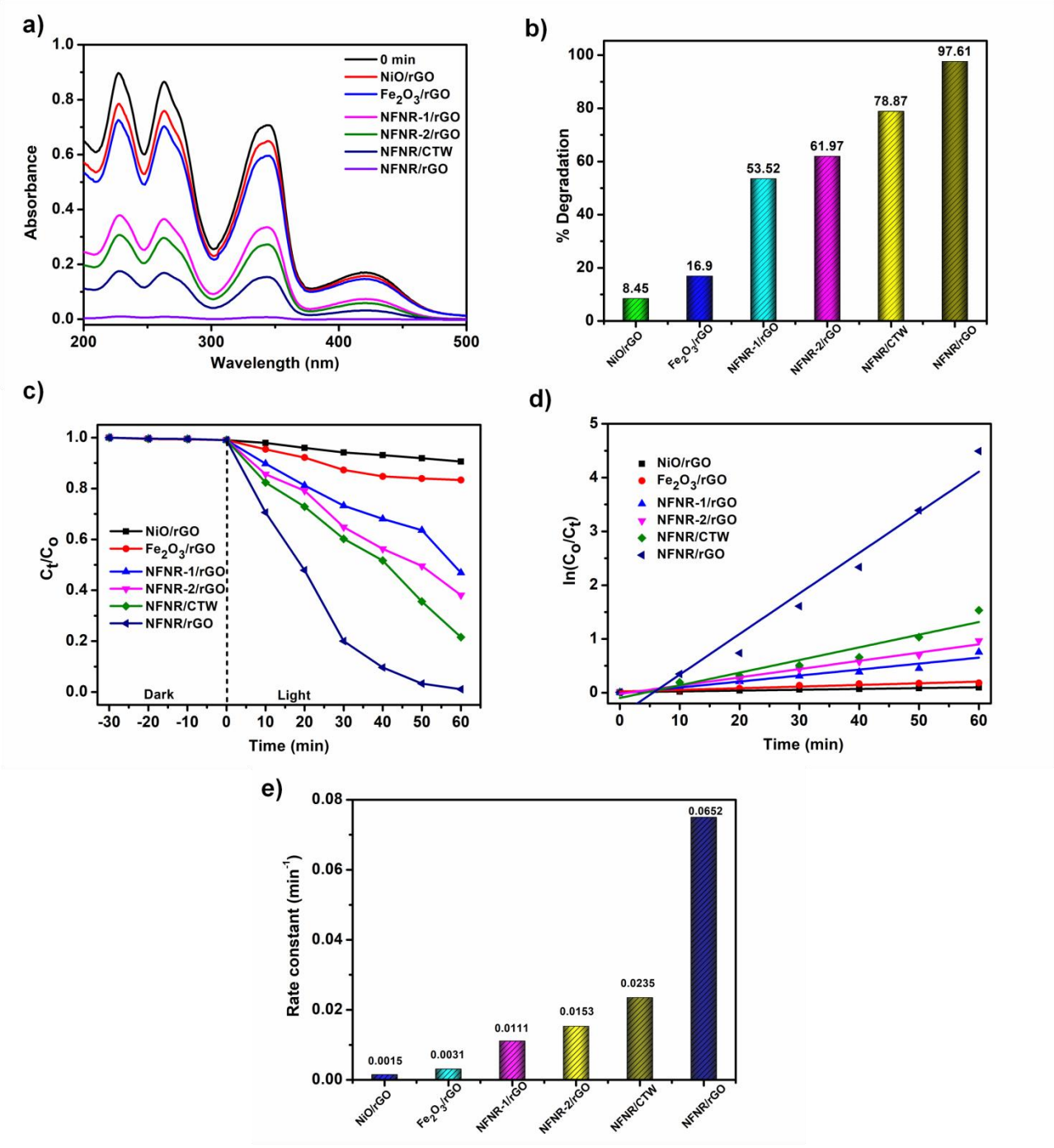

Fig. S21 a) Absorption spectra and b) % degradation of the BH solution over different catalyst under UV-light irradiation; c) photocatalytic degradation of BH solution under UV-light irradiation, d) corresponding photodegradation kinetic curves, e) rate constant of BH removal over as-prepared catalysts. (20 ml of 50 ppm BH solution, 12 mg catalyst, pH=2 and 60 min irradiation time).

24.

Table S3 Comparative study of the efficiency of Nickel ferrite photocatalysts for organic pollutants degradation.

Entry No	Photocatalysts[a]	Pollutants	Efficiency	Light source	Time	Ref
1	Nickel ferrite-carbon nanoflakes (NiFe@NCF) nanocomposite	LEV CIP	99.91% 98.86%	Visible light	50 min 70 min	[12]
2	$NiFe_2O_4$-Ag-ZnO	Methylene Blue (MB) dye	98 %	UV-light	60 min	[13]
3	$NiFe_2O_4$	MB	~98.5 %	UV/Vis light	70 min	[14]
4	$gC_3N_4/NiFe_2O_4/Ag$	Tetracycline	92.1 %	Visible light	120 min	[15]
5	nickel ferrite/zinc oxide ($NiFe_2O_4$/ZnO)	Methyl orange Methyl blue Crystal violet	49.2% 44.4% 41.3%	Solar light	40 min	[16]
6	$NiFe_2O_4$	MG dye Pharmaceutical SSX	99% 74%		120 min	[17]
7	Nickel ferrite/chitosan/bismuth(III) oxyiodide	Metronidazole	100%	Sunlight	200 min	[18]
8	MWCNT–$CuNiFe_2O_4$	Acid blue 113 (AB113) dye	100 %	UV light	30 min	[19]
9	Ni@$NiFe_2O_4$/ZnO	β-lactam antibiotic - cefadroxil	95 %	Solar light	60 min	[20]
10	Cd-Gd-doped nickel spinel ferrite/rGO	Methylene Blue Rhodamine-B	92.27% 53.18%	Visible light	120 min	[21]
11	**$NiFe_2O_4$/rGO (NFNR/rGO)**	**Berberine hydrochloride (BH)**	**97.61 %**	**UV-light**	**60 min**	**This study**

[a] $NiFe_2O_4$ based reported photocatalysts considered here for comparison.

References

1 J.L. Ortiz-Quiñonez, U. Pal and M.S. Villanueva, *ACS Omega*, 2018, **3**, 14986-15001.

2 S. Mishra, P. Kumar and S.K. Samanta, *Ind. Eng. Chem. Res.*, 2020, **59**, 15839-15847.

3 K.K.H. De Silva, P. Viswanath, V.K. Rao, S. Suzuki and M. Yoshimura, *J. Phys. Chem. C*, 2021, **125**, 7791-7798.

4 M. Qayoom, K.A. Shah, A.H. Pandit, A. Firdous and G.N. Dar, *J. Electroceram.*, 2020, **45**, 7-14.

5 H. Mansour, H. Letifi, R. S. Bargougui, De Almeida-Didry, B. Negulescu, C. Autret-Lambert, A. Gadri and S. Ammar, *Appl. Phys. A*, 2017, **123**, 1-10.

6 J. Qiu, T.H. Nguyen, S. Kim, Y.J. Lee, M.T. Song, W.J. Huang, X.B. Chen, T.M.H. Nguyen and I.S. Yang, *Spectrochim. Acta, Part A*, 2022, **280**, 121498.

7 M. Shabani, E. Saebnoori, S.A. Hassanzadeh-Tabrizi and H.R. Bakhsheshi-Rad, *J. Mater. Sci.: Mater. Electron.*, 2021, **32**, 10424-10442.

8 Z. Iqbal, M.S. Tanweer and M. Alam, *ACS Omega*, 2023, **8**, 6376-6390.

9 M. Shabani, E. Saebnoori, S.A. Hassanzadeh-Tabrizi and H.R. Bakhsheshi-Rad, *J. Mater. Sci.: Mater. Electron.*, 2021, **32**, 10424-10442.

10 L.T.M. Thy, N.T.C. Linh, N.T.T. Tram, T.H. Tu, L.T. Tai, P.T. Khang, H.M. Nam, N.H. Hieu and M.T. Phong, *J. Nanomater.*, 2021, **2021**, 4636531.

11 M. Farahmandjou and F. Soflaee, *Phys. Chem. Res.*, 2015, **3**, 191-196.

12 S. Patar, R. Mittal, F. Yasmin, B.K. Bhuyan and L.J. Borthakur, *Chemosphere*, 2024, **363**, 142908.

13 A. Singh, F. Wan, K. Yadav, S. Kharbanda, P. Thakur and A. Thakur, *Mater. Sci. Eng. B*, 2024, **299**, 116935.

14 W.M. Alamier, N. Hasan, M.S. Nawaz, K.S. Ismail, M. Shkir, M.A. Malik and M.D. Oteef, *J. Mater. Res. Technol.*, 2023, **22**, 1331-1348.

15 S.A. Hassanzadeh-Tabrizi, *J. Photochem. Photobiol., A,* 2021, **418**, 113398.

16 S. Munir, M.F. Warsi, S. Zulfiqar, I. Ayman, S. Haider, I.A. Alsafari, P.O. Agboola and I. Shakir, *J. Saudi Chem. Soc.*, 2021, **25**, 101388.

17 A. Makofane, P.J. Maake, M.M. Mathipa, N. Matinise, F.R. Cummings, D.E. Motaung and N.C. Hintsho-Mbita, *Inorg. Chem. Commun.*, 2022, **139**, 109348.

18 F.S. Arghavan, T.J. Al-Musawi, G.A. Rumman, R. Pelalak, A. Khataee and N. Nasseh, *J. Environ. Chem. Eng.*, 2021, **9**, 105619.

19 T.J. Al-Musawi, N. Mengelizadeh, M. Taghavi, Z. Shehu and D. Balarak, *Environ. Sci. Pollut. Res.*, 2022, **29**, 51703-51716.

20 S.S.M. Thaha, N. Pugazhenthiran, P. Sathishkumar, V.T. Perarasu, R. Kumaresan, M.A. Assiri and M. Selvaraj, *Ceram. Int.*, 2024.

21 A. Rahman, S. Zulfiqar, A.U. Haq, I.A. Alsafari, U.Y. Qazi, M.F. Warsi and M. Shahid, *Ceram. Int.*, 2021, **47**, 9513-9521.